Journal of Sound and Vibration (2001) **245**(2), 261–283
doi:10.1006/jsvi.2000.3560, available online at http://www.idealibrary.com on IDEAL®

VIBRATIONS OF CIRCULAR PLATES RESTING ON A SLOSHING LIQUID: SOLUTION OF THE FULLY COUPLED PROBLEM

M. Amabili

Dipartimento di Ingegneria Industriale, University of Parma, Parco Area delle Scienze 181/*A*, 43100 *Parma, Italy. E-mail: marco@me.unipr.it*

(*Received* 17 *August* 2000, *and in final form* 5 *December* 2000)

Vibrations of circular plates resting on a sloshing liquid free surface are studied. The fully coupled problem between sloshing modes of the free surface and bulging modes of the plate is solved by using the Rayleigh–Ritz method. The sloshing boundary condition is directly inserted into the eigenvalue problem. The liquid domain is limited by a rigid cylindrical surface and a rigid flat bottom. The fluid is considered inviscid and incompressible; it is described by the velocity potential expanded in a series. The present model has as limit cases: (1) circular plates resting on half-infinite liquid domain and (2) circular plates completely covering the liquid in a circular cylindrical tank. The theory is suitable for all axisymmetric plate boundary conditions. The effect of free surface waves on the plate natural frequencies is significant when the fundamental bulging mode of the plate has its natural frequency close to those of the first sloshing modes of the free surface. The present original solution allows the study of plates having a very strong coupling between sloshing and bulging modes to be studied to a high level of accuracy. The convergence of the method is shown. The natural frequencies and mode shapes for different system parameters are given.

1. INTRODUCTION

Vibrations of circular plates coupled to liquids have been studied since the pioneering work of Lord Rayleigh [1]. Lamb [2] studied the free vibrations of clamped, circular baffled plates in contact with a semi-infinite fluid volume on one side. Lamb used simple assumed modes and an approximation to obtain the hydrodynamic pressure; this solution was extended to free-edge circular plates by McLachlan [3]. Recently, Amabili and Kwak [4] have re-analyzed the same problem by using a refined approach based on the Hankel transformation; the solution was obtained for any boundary condition uniform around the plate edge. The effect of a finite fluid depth above the baffled plate was investigated by Amabili [5]. The free surface of the liquid was present but free-surface waves were neglected. Amabili *et al.* [6] extended the study in reference [4] to annular, baffled plates. For this class of problems, the boundary conditions on the fluid domain are homogeneous and give rise to a Neumann problem. Circular baffled plates have also been studied by Ginsberg and Chu [7]; they considered circular plates in both an infinite or annular baffle, completely immersed in fluid.

Circular plates coupled to a liquid with a free surface give a system with two families of natural modes: sloshing and bulging ones. Sloshing modes are caused by the oscillation of the liquid free surface. Their modal properties are characterized by the shape of the liquid domain and much less by the flexibility of the coupled structure; sloshing modes are also

0022-460X/01/320261 + 23 $35.00/0

present in rigid containers. The bulging modes are the vibrations of the structure that are affected by the fluid–structure interaction. In particular, for low-frequency modes, the fluid–structure interaction gives an added mass effect to the system, thus lowering the natural frequencies of the bulging modes. When the fundamental bulging mode of the plate has its natural frequency close to those of the first sloshing modes of the free surface of the liquid, very large coupling between the two families of modes arises and it can be difficult to distinguish between sloshing and bulging modes. Only bulging modes can be studied whilst neglecting free-surface waves.

Elastic circular bottom plates in fluid-filled cylindrical tanks have been largely studied in relation to plate vibrations and fluid sloshing in the container, e.g., see references [8–22]. In this case, the fluid velocity potential can be obtained by using the method of separation of variables. In particular, Bhuta and Koval [8] were the first to solve the coupled problem of fluid sloshing and plate oscillation. Tong [9] inserted the effect of surface tension. Bauer *et al.* [12] studied the effect of the large amplitude of surface waves. This effect was experimentally and theoretically investigated by Chiba [15, 17, 18]. Nagaya and Nagai [14] included the viscosity of the liquid and an elastic foundation under the plate. Amabili *et al.* [22] considered a complete elastic tank, composed of a circular cylindrical shell and a bottom plate resting on an elastic foundation, containing a sloshing liquid. Amabili and Dalpiaz [21] studied, theoretically and experimentally, annular bottom plates, neglecting free-surface waves in the theory.

Bauer [23] studied a circular plate completely covering the liquid surface in an otherwise rigid cylindrical tank. The liquid was considered inviscid and incompressible.

Free vibrations of circular plates resting on a free liquid surface were studied for the first time by Kwak and Kim [24] for axisymmetric modes and by Kwak [25] for the general case. The liquid coupled to the plate was considered semi-infinite. These studies also address circular plates completely submerged in an infinite fluid domain. Experiments confirming the results of references [24, 25] have been performed by Amabili *et al.* [26]. Kwak and Amabili [27] extended this study to annular plates, successfully comparing the theoretical and experimental results. The effect of finite fluid depth under the plate was theoretically and experimentally studied by Kwak and Han [28], but in the model the fluid was assumed to be infinite in the radial direction. In all these models [24–28], the boundary conditions on the fluid domain were mixed and gave rise to a Dirichlet problem. In particular, a zero velocity potential was imposed at the free liquid surface, so that the effect of free-surface waves was neglected and only bulging modes were investigated. Amabili and Kwak [29] studied the effect of free-surface waves on the natural frequency of bulging modes by using a perturbation approach; however, sloshing modes cannot be studied with this method.

Vibrations of circular plates resting on a sloshing liquid free surface are studied in the present paper. Free-edge circular plates floating on a liquid surface can be used to control the dangerous sloshing of propellant in rockets with the exception of the first asymmetric mode. To control this mode, a circular plate with a restrained displacement at the edges (clamped or simply supported) must be used. This plate can be guided, such that the plate can move perpendicular to the axis of the container, to float on the propellant surface when its level decreases. Other applications are related to nuclear and naval engineering. The fully coupled problem between sloshing modes of the free surface and bulging modes of the plate is solved by using the Rayleigh–Ritz method. The sloshing boundary condition is directly inserted into the eigenvalue problem. The liquid domain is limited by a rigid cylindrical surface and a rigid flat bottom. The fluid is considered inviscid and incompressible; it is described by the velocity potential that is expanded in a series. The present model gives as limit cases: (1) circular plates resting on a half-infinite liquid domain and (2) circular plates completely covering the liquid in a circular cylindrical tank. These cases have been studied

previously by Kwak [25], neglecting free surface waves, and Bauer [23]. This allows for a comparison of the results and the validation of the present study. The theory is suitable for all axisymmetric plate boundary conditions. The effect of free-surface waves on the plate's natural frequencies is significant when the fundamental bulging mode of the plate has its natural frequency close to those of the first sloshing modes of the free surface. The case of very strong interaction between sloshing and bulging modes is solved and indicates the high degree of accuracy of the present approach even in this critical condition. Interesting phenomena are detected when a strong interaction between sloshing and bulging modes arises. Convergence of the method is shown and the results for different system parameters are given.

2. KINETIC AND POTENTIAL ENERGY OF THE PLATE

A polar co-ordinate system (O, r, θ) is introduced with the origin O at the centre of the plate. The mode shapes, related to the transverse deflection w, for free vibrations of thin elastic circular plates coupled to the liquid are expanded by using as admissible functions the *in vacuo* eigenfunctions

$$w(r, \theta) = \sum_{m=0}^{\infty} q_m W_{nm}(r) \cos(n\theta), \tag{1}$$

where

$$W_{nm}(r) = [A_{nm} \mathrm{J}_n(\lambda_{nm} r/a) + C_{nm} \mathrm{I}_n(\lambda_{nm} r/a)], \tag{2}$$

q_m are the Ritz unknown coefficients, n is the number of nodal diameters, m the number of nodal circles, λ_{nm} the frequency parameter and A_{nm} and C_{nm} are the mode-shape parameters; the frequency and mode-shape parameters depend on the plate's boundary conditions. J_n and I_n are the Bessel function and the modified Bessel function of order n respectively. The equations that give λ_{nm} and A_{nm}/C_{nm} are given in Appendix A. The admissible functions are linearly independent and constitute a complete set. In equation (1) only modes with a different number of nodal circles are coupled by the liquid–plate interaction; for symmetry reason (see Figure 1), there is no coupling among modes having a different number of nodal

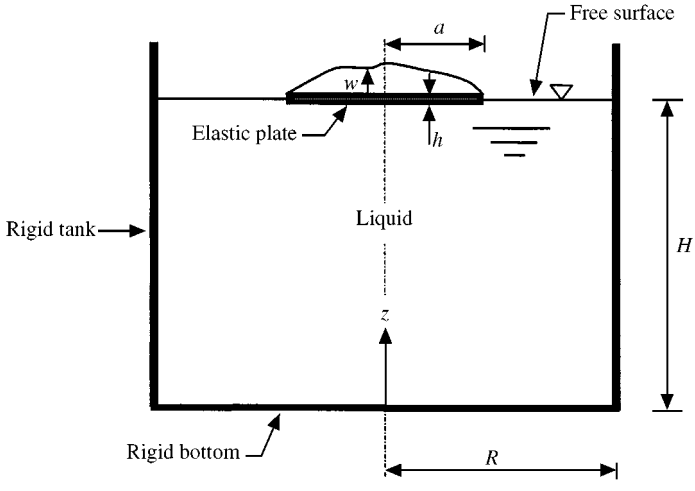

Figure 1. Elastic circular plate on liquid surface.

diameters. The radian *in vacuo* frequency of vibration ω_{nm} and the frequency parameter λ_{nm} are related by

$$\omega_{nm} = \lambda_{nm}^2 \sqrt{D/(\rho_P h a^4)}, \tag{3}$$

where $D = (Eh^3)/[12(1-\nu^2)]$, ρ_P is the plate mass density, h the plate thickness, a the plate radius, E the Young's modulus and ν the Poisson ratio. In equation (1) the Kirchhoff theory of plates was used. To simplify the computations, the mode-shape parameters A_{nm} and C_{nm} are normalized in order to have (see equations (11.106), (33.101) and (31.101) in reference [30])

$$\begin{aligned}\int_0^1 &[A_{nm}\,\mathrm{J}_n(\lambda_{nm}\rho) + C_{nm}\,\mathrm{I}_n(\lambda_{nm}\rho)]^2\,\rho\,\mathrm{d}\rho \\ &= \left\{\frac{A_{nm}^2}{2}\left[(\mathrm{J}_n'(\lambda_{nm}))^2 + \left(1-\frac{n^2}{\lambda_{nm}^2}\right)\mathrm{J}_n^2(\lambda_{nm})\right] - \frac{C_{nm}^2}{2}\left[(\mathrm{I}_n'(\lambda_{nm}))^2 - \left(1+\frac{n^2}{\lambda_{nm}^2}\right)\mathrm{I}_n^2(\lambda_{nm})\right]\right. \\ &\quad \left. + \frac{A_{nm}C_{nm}}{\lambda_{nm}}\left[\mathrm{J}_n(\lambda_{nm})\,\mathrm{I}_{n+1}(\lambda_{nm}) + \mathrm{I}_n(\lambda_{nm})\,\mathrm{J}_{n+1}(\lambda_{nm})\right]\right\} = 1,\end{aligned} \tag{4}$$

where $\rho = r/a$ and J_n' and I_n' indicate the derivatives of J_n and I_n with respect to the argument.

The reference kinetic energy T_P^* of the plate is given by

$$T_P^* = \frac{1}{2}\rho_P h \int_0^{2\pi}\int_0^a w^2\, r\,\mathrm{d}r\,\mathrm{d}\theta = \frac{1}{2}\rho_P\, a^2\, h\,\psi_n \sum_{m=0}^{\infty} q_m^2, \tag{5}$$

where

$$\psi_n = \begin{Bmatrix} 2\pi & \text{if } n=0 \\ \pi & \text{if } n>0 \end{Bmatrix}.$$

In equation (5) the orthogonality of Bessel functions (plate mode shapes) has been used.

For each mode of the plate vibrating *in vacuo*

$$\omega_{nm}^2 = \frac{V_P}{T_P^*}, \tag{6}$$

where V_P is the maximum potential energy of the plate and T_P^* its reference kinetic energy calculated for that specific mode; for each *in vacuo* mode, $V_P = \omega_{nm}^2 T_P^*$. Therefore, the maximum potential energy of the plate coupled to the liquid is the sum of the reference kinetic energies of the *in vacuo* modes of the plate multiplied by ω_{nm}^2, i.e.,

$$V_P = \frac{1}{2}\rho_P\, a^2\, h\,\psi_n \sum_{m=0}^{\infty} q_m^2\,\omega_{nm}^2 = \frac{1}{2}\frac{D}{a^2}\,\psi_n \sum_{m=0}^{\infty} q_m^2\,\lambda_{nm}^4. \tag{7}$$

3. VELOCITY POTENTIAL OF THE LIQUID

For an incompressible and inviscid liquid, it is possible to describe the irrotational liquid motion (due to the plate's vibration) by means of the velocity potential Φ that must satisfy the Laplace equation $\nabla^2\Phi = 0$. The velocity of the liquid is given by $\mathbf{v} = \nabla\Phi$. A cylindrical co-ordinate system (z, r, θ) is introduced as shown in Figure 1; R is the inner radius of the

rigid cylindrical tank and H the liquid level. By using the variable separation with respect to the angular co-ordinate, Φ can be expressed as

$$\Phi(r, \theta, z) = \phi_{nm}(r, z) \cos(n\theta), \tag{8}$$

where ϕ_{nm} satisfies

$$\frac{\partial^2 \phi_{nm}}{\partial r^2} + \frac{\partial \phi_{nm}}{r \partial r} + \frac{\partial^2 \phi_{nm}}{\partial z^2} - \frac{n^2}{r^2} \phi_{nm} = 0. \tag{9}$$

Then, the following is imposed: (1) contact without cavitation at the liquid-rigid bottom interface; (2) contact without cavitation at the liquid-rigid lateral cylindrical interface; (3) contact without cavitation at the liquid–plate interface, for $0 \leqslant r \leqslant a$; and (4) the linearized sloshing condition at the free surface of the liquid, for $a < r \leqslant R$ (see Figure 1). The superficial tension of the fluid is neglected. Therefore, the boundary conditions are expressed by

$$\left.\frac{\partial \Phi}{\partial z}\right|_{z=0} = 0, \quad \text{which gives} \left.\frac{\partial \phi_{nm}}{\partial z}\right|_{z=0} = 0, \tag{10}$$

$$\left.\frac{\partial \Phi}{\partial r}\right|_{r=R} = 0, \quad \text{which gives} \left.\frac{\partial \phi_{nm}}{\partial r}\right|_{r=R} = 0, \tag{11}$$

$$\left.\frac{\partial \Phi}{\partial z}\right|_{z=H} = \left\{ \begin{matrix} w & \text{for } 0 \leqslant r \leqslant a \\ \dfrac{\omega^2}{g} \Phi|_{z=H} & \text{for } a < r \leqslant R \end{matrix} \right\}, \tag{12}$$

where g is the gravity acceleration and ω is the circular frequency of vibration of the coupled system.

The solution of equation (9) in the circular cylindrical fluid domain is

$$\phi_{nm} = a_0 + \sum_{m=1}^{\infty} \mathrm{J}_n(\varepsilon_{nm} r/R)[a_{nm} \cosh(\varepsilon_{nm} z/R) + b_{nm} \sinh(\varepsilon_{nm} z/R)], \tag{13}$$

where J_n is the Bessel function of order n and a_0 is equal to zero for $n > 0$. The modified Bessel function I_n was discharged in equation (13) because it cannot satisfy the boundary condition given by equation (11).

Equation (10) is satisfied by taking

$$b_{nm} = 0; \tag{14}$$

equation (11) is satisfied by ε_{nm} being the roots of the following equation:

$$\mathrm{J}'_n(\varepsilon_{nm}) = 0; \tag{15}$$

if $n = 0$, the first root is zero, i.e., $\varepsilon_{00} = 0$, which is associated with the term a_0 in equation (13). It is convenient to rewrite equation (13) in a slightly different form, obtained by multiplying the previous unknown parameters a_{nm} by the quantity $\cosh(\varepsilon_{nm} H/R)$:

$$\phi_{nm} = a_0 + \sum_{m=1}^{\infty} a_{nm} \mathrm{J}_n(\varepsilon_{nm} r/R) \cosh(\varepsilon_{nm} z/R)/\cosh(\varepsilon_{nm} H/R). \tag{16}$$

Equation (16) is the solution of the boundary value problem but it must satisfy the last boundary condition given by equation (12). Substitution of equations (8) and (16) into equation (12), multiplying by $(1/R^2)\,\mathrm{J}_n(\varepsilon_{nk}\,r/R)\,r\,\mathrm{d}r$ and integrating between 0 and R gives

$$\frac{\varepsilon_{nk}}{R}\,a_{nk}\,\alpha_{nk}\tanh\left(\varepsilon_{nk}\,\frac{H}{R}\right)\cos(n\,\theta)=\frac{1}{R^2}\left\{\int_0^a w\,\mathrm{J}_n\left(\varepsilon_{nk}\,\frac{r}{R}\right)r\,\mathrm{d}r+\frac{\omega^2}{g}\int_a^R \Phi|_{z=H}\,\mathrm{J}_n\left(\varepsilon_{nk}\,\frac{r}{R}\right)r\,\mathrm{d}r\right\}$$

$$\text{for } k=1,\ldots,\infty, \tag{17a}$$

where α_{nk} is defined by the following expression [30]:

$$\frac{1}{R^2}\int_0^R \mathrm{J}_n\left(\varepsilon_{nm}\,\frac{r}{R}\right)\mathrm{J}_n\left(\varepsilon_{nk}\,\frac{r}{R}\right)r\,\mathrm{d}r=\alpha_{nk}\delta_{mk}=(1/2)\left[1-(n/\varepsilon_{nk})^2\right]\left[\mathrm{J}_n(\varepsilon_{nk})\right]^2\delta_{mk} \tag{18}$$

and δ_{mk} is the Kronecker delta. Equation (17a) determines the unknown parameters a_{nk}. For $n=0$ the following equation ($k=0$) must be added to equation (17a) due to the presence of the constant term a_0:

$$0=\frac{1}{R^2}\left\{\int_0^a wr\,\mathrm{d}r+\frac{\omega^2}{g}\int_a^R \Phi|_{z=H}\,r\,\mathrm{d}r\right\}. \tag{17b}$$

By using equations (1), (8) and (16), the set of equations (17) can be rewritten in the form

$$R\,\varepsilon_{nk}\,a_{nk}\,\alpha_{nk}\tanh\left(\varepsilon_{nk}\,\frac{H}{R}\right)=\sum_{m=0}^{\infty}q_m\int_0^a W_{nm}(r)\,\mathrm{J}_n\left(\varepsilon_{nk}\,\frac{r}{R}\right)r\,\mathrm{d}r$$

$$+\frac{\omega^2}{g}\left[\sum_{m=1}^{\infty}a_{nm}\int_a^R \mathrm{J}_n\left(\varepsilon_{nm}\,\frac{r}{R}\right)\mathrm{J}_n\left(\varepsilon_{nk}\,\frac{r}{R}\right)r\,\mathrm{d}r+a_0\int_a^R \mathrm{J}_0\left(\varepsilon_{0k}\,\frac{r}{R}\right)r\,\mathrm{d}r\right]\quad\text{for } k=1,\ldots,\infty \tag{19a}$$

and for $n=0$ the following equation must be added:

$$0=\sum_{m=0}^{\infty}q_m\int_0^a W_{0m}(r)\,r\,\mathrm{d}r+\frac{\omega^2}{g}\left[\sum_{m=1}^{\infty}a_{0m}\int_a^R \mathrm{J}_0\left(\varepsilon_{0m}\,\frac{r}{R}\right)r\,\mathrm{d}r+a_0\int_a^R r\,\mathrm{d}r\right]. \tag{19b}$$

The following parameters, related to integrals in the set of equations (19), are introduced [30, 31]:

$$\bar{\alpha}_{nk}=\int_0^a\left[\mathrm{J}_n(\varepsilon_{nk}\,r/R)\right]^2 r\,\mathrm{d}r$$

$$=\frac{a^2}{2}\left\{\left[\mathrm{J}_n'(\varepsilon_{nk}\,a/R)\right]^2+\left(1-\frac{n^2}{\varepsilon_{nk}^2\,a^2/R^2}\right)\left[\mathrm{J}_n(\varepsilon_{nk}\,a/R)\right]^2\right\}, \tag{20}$$

$$\eta_{nmk}=-\int_0^a \mathrm{J}_n(\varepsilon_{nm}\,r/R)\,\mathrm{J}_n(\varepsilon_{nk}\,r/R)\,r\,\mathrm{d}r$$

$$=\frac{Ra}{\varepsilon_{nm}^2-\varepsilon_{nk}^2}\left[\varepsilon_{nm}\,\mathrm{J}_{n-1}(\varepsilon_{nm}\,a/R)\,\mathrm{J}_n(\varepsilon_{nk}\,a/R)-\varepsilon_{nk}\,\mathrm{J}_{n-1}(\varepsilon_{nk}\,a/R)\,\mathrm{J}_n(\varepsilon_{nm}\,a/R)\right], \tag{21}$$

$$\beta_{nmk} = \int_0^a \mathrm{J}_n(\lambda_{nm} r/a)\, \mathrm{J}_n(\varepsilon_{nk} r/R)\, r\, \mathrm{d}r$$

$$= \frac{Ra^2[R\,\lambda_{nm}\,\mathrm{J}_n(\varepsilon_{nk} a/R)\,\mathrm{J}_{n-1}(\lambda_{nm}) - a\,\varepsilon_{nk}\,\mathrm{J}_{n-1}(\varepsilon_{nk} a/R)\,\mathrm{J}_n(\lambda_{nm})]}{a^2\,\varepsilon_{nk}^2 - R^2\lambda_{nm}^2}, \tag{22}$$

$$\gamma_{nmk} = \int_0^a \mathrm{I}_n(\lambda_{nm} r/a)\, \mathrm{J}_n(\varepsilon_{nk} r/R)\, r\, \mathrm{d}r$$

$$= \frac{Ra^2[R\,\lambda_{nm}\,\mathrm{J}_n(\varepsilon_{nk} a/R)\,\mathrm{I}_{n+1}(\lambda_{nm}) + a\,\varepsilon_{nk}\,\mathrm{J}_{n+1}(\varepsilon_{nk} a/R)\,\mathrm{I}_n(\lambda_{nm})]}{a^2\,\varepsilon_{nk}^2 + R^2\lambda_{nm}^2}. \tag{23}$$

Equation (21) is valid for $m \neq k$. By using equations (18), (20) and (21) the following integral is obtained:

$$\int_a^R \mathrm{J}_n(\varepsilon_{nm} r/R)\,\mathrm{J}_n(\varepsilon_{nk} r/R)\, r\, \mathrm{d}r = \begin{Bmatrix} R^2\alpha_{nk} - \bar{\alpha}_{nk} & \text{if } m = k \\ \eta_{nmk} & \text{if } m \neq k \end{Bmatrix}. \tag{24}$$

Moreover,

$$\int_a^R \mathrm{J}_0(\varepsilon_{0k} r/R)\, r\, \mathrm{d}r = (R/\varepsilon_{0k})[R\,\mathrm{J}_1(\varepsilon_{0k}) - a\,\mathrm{J}_1(\varepsilon_{0k} a/R)]. \tag{25}$$

By using equations (22)–(25), the boundary condition given by equation (19) can be written in the final form

$$R\,\varepsilon_{nk}\,a_{nk}\,\alpha_{nk}\tanh\left(\varepsilon_{nk}\frac{H}{R}\right) - \sum_{m=0}^{\infty} q_m(A_{nm}\beta_{nmk} + C_{nm}\gamma_{nmk})$$

$$= \frac{\omega^2}{g}\left\{\sum_{m=1}^{\infty} a_{nm}[(R^2\alpha_{nk} - \bar{\alpha}_{nk})\,\delta_{mk} + (1-\delta_{mk})\,\eta_{nmk}]\right.$$

$$\left. + a_0\,(R/\varepsilon_{0k})[R\,\mathrm{J}_1(\varepsilon_{0k}) - a\,\mathrm{J}_1(\varepsilon_{0k} a/R)]\right\} \quad \text{for } k = 1, \ldots, \infty. \tag{26a}$$

In equation (26) $a_0 = 0$ if $n > 0$. If $n = 0$, the following equation must be added to the set of boundary conditions given by (26a)

$$-a^2 \sum_{m=0}^{\infty} q_m = \frac{\omega^2}{g}\left\{\sum_{m=1}^{\infty} a_{0m}(R/\varepsilon_{0m})[R\mathrm{J}_1(\varepsilon_{0m}) - a\mathrm{J}_1(\varepsilon_{0m} a/R)] + a_0(R^2 - a^2)/2\right\}. \tag{26b}$$

The boundary condition given by equations (26a) and (b) will be used in the eigenvalue problem to obtain the unknown parameters a_{nm}.

4. KINETIC ENERGY OF THE LIQUID

For a plate vibrating on the fluid free surface one has [32, 33]

$$\omega_F^2 = (V_P + V_F)/(T_P^* + \tilde{T}_F^*), \tag{27}$$

where T_P^* and V_P are given in equations (5) and (7), V_F is the maximum potential energy associated to free-surface waves and $\tilde{T}_F^*$ is the reference kinetic energy of the fluid; ω_F is the circular frequency of the natural free vibration of the plate resting on the liquid. It is well known that by using Green's theorem [32–34] it is possible to evaluate the reference kinetic energy of the fluid with a surface integral on the boundary of the fluid domain, where the contribution of rigid surfaces delimiting the fluid domain is zero. Amabili [32, 33] proved that equation (27) can be simplified into

$$\omega_F^2 = V_P/(T_P^* + T_F^*), \tag{28}$$

where T_F^* is the reduced reference kinetic energy of the fluid computed by integrating only over the wet plate surface.

The reduced reference kinetic energy of the fluid is expressed as

$$\begin{aligned} T_F^* &= \frac{1}{2}\rho_F \int_0^{2\pi}\int_0^a \Phi|_{z=H}(\partial\Phi/\partial z)|_{z=H}\, r\,\mathrm{d}r\,\mathrm{d}\theta \\ &= \frac{1}{2}\rho_F \int_0^{2\pi}\int_0^a \Phi|_{z=H}\, wr\,\mathrm{d}r\,\mathrm{d}\theta \\ &= \frac{1}{2}\rho_F\psi_n\left[\sum_{m=0}^{\infty}\sum_{k=1}^{\infty} q_m a_{nk}\int_0^a \mathrm{J}_n(\varepsilon_{nk} r/R)\, W_{nm}\, r\,\mathrm{d}r + a_0\sum_{m=0}^{\infty} q_m\int_0^a W_{0m}\, r\,\mathrm{d}r\right] \\ &= \frac{1}{2}\rho_F\psi_n\left[\sum_{m=0}^{\infty}\sum_{k=1}^{\infty} q_m a_{nk}\,(A_{nm}\beta_{nmk} + C_{nm}\gamma_{nmk}) + a_0 a^2\sum_{m=0}^{\infty} q_m\right], \end{aligned} \tag{29}$$

where ρ_F is the mass density of the liquid. Equation (29) has been obtained by using equations (4) and (12). If $n > 0$, the term including a_0 vanishes.

5. EIGENVALUE PROBLEM

For the numerical calculation of the natural frequencies and modes, only N_1 terms in the expansion of w, equation (1), and N_2 terms (actually $N_2 + 1$ terms for $n = 0$) in the expansion of Φ, equations (8) and (13), are considered, where N_1 and N_2 are chosen large enough to give the required accuracy to the solution. All the energies are given by finite summations. It is convenient to introduce a vectorial notation. The vector $\mathbf{q}$ of the parameters of the Ritz expansion is defined by

$$\mathbf{q}^{\mathrm{T}} = \{q_0, \ldots, q_{N_1-1}\}. \tag{30}$$

The maximum potential energy of the bottom plate, equation (7), can be written as

$$V_P = \tfrac{1}{2}\psi_n \mathbf{q}^{\mathrm{T}}\mathbf{K}_P\mathbf{q}, \tag{31}$$

where the elements of the diagonal matrix $\mathbf{K}_P$ are given by

$$[\mathbf{K}_P]_{mi} = \delta_{mi}(D/a^2)\lambda_{nm}^4, \quad m, i = 0, \ldots, N_1 - 1 \tag{32}$$

and δ_{mi} is the Kronecker delta.

The reference kinetic energy of the plate, equation (5), may be written as

$$T_P^* = \tfrac{1}{2}\,\psi_n\,\mathbf{q}^{\mathrm{T}}\mathbf{M}_P\,\mathbf{q}, \tag{33}$$

where

$$[\mathbf{M}_P] = \rho_P\,h\,a^2[\mathbf{I}], \tag{34}$$

and $[\mathbf{I}]$ is the $N_1 \times N_1$ identity matrix.

The vector $\mathbf{a}$ of the parameters in the expansion of the velocity potential of the liquid is defined as

$$\mathbf{a}^{\mathrm{T}} = \{a_{n0}, a_{n1}, \ldots, a_{n,N_2}\}, \tag{35}$$

where a_{n0} must be eliminated by equation (30) for $n > 0$.

The reference kinetic energy of the fluid, equation (29), can be written in a vectorial notation

$$T_F^* = \tfrac{1}{2}\,\psi_n\,\mathbf{q}^{\mathrm{T}}\mathbf{M}_F\,\mathbf{a}, \tag{36}$$

where

$$[\mathbf{M}_F]_{mi} = \rho_F(A_{nm}\,\beta_{nmi} + C_{nm}\,\gamma_{nmi}), \quad m = 0, \ldots, N_1 - 1 \quad \text{and} \quad i = 1, \ldots, N_2; \tag{37a}$$

if $n = 0$, the following column must be added to matrix $\mathbf{M}_F$

$$[\mathbf{M}_F]_{m0} = \rho_F\,a^2, \quad m = 0, \ldots, N_1 - 1. \tag{37b}$$

The boundary condition given by equation (26) is directly inserted in the eigenvalue problem and therefore it is transformed into the following vectorial notation:

$$\mathbf{K}_1\mathbf{q} + \mathbf{K}_S\,\mathbf{a} - \omega^2\mathbf{M}_S\,\mathbf{a} = 0, \tag{38}$$

where

$$\mathbf{K}_1 = -\,\mathbf{M}_F^{\mathrm{T}}, \tag{39}$$

$$[\mathbf{K}_S]_{mi} = \rho_F\,R\varepsilon_{nm}\alpha_{nm}\tanh(\varepsilon_{nm}\,H/R)\,\delta_{mi}, \quad m, i = 0, \ldots, N_2, \tag{40}$$

$$[\mathbf{M}_S]_{mi} = (\rho_F/g)\,[(R^2\,\alpha_{nm} - \bar{\alpha}_{nm})\,\delta_{mi} + (1 - \delta_{mi})\,\eta_{nmi}], \quad m, i = 1, \ldots, N_2; \tag{41a}$$

if $n = 0$, the following row and column must be added to matrix $\mathbf{M}_S$:

$$[\mathbf{M}_S]_{00} = (\rho_F/g)(R^2 - a^2)/2, \tag{41b}$$

$$[\mathbf{M}_S]_{m0} = (\rho_F/g)\,(R/\varepsilon_{0m})\,[R\mathrm{J}_1(\varepsilon_{0m}) - a\,\mathrm{J}_1(\varepsilon_{0m}a/R)], \quad m = 1, \ldots, N_2, \tag{41c}$$

$$[\mathbf{M}_S]_{0i} = (\rho_F/g)\,(R/\varepsilon_{0i})\,[R\mathrm{J}_1(\varepsilon_{0i}) - a\,\mathrm{J}_1(\varepsilon_{0i}a/R)], \quad i = 1, \ldots, N_2. \tag{41d}$$

In particular, all terms in equation (28) have been multiplied by ρ_F with respect to those given in equation (26) in order to obtain a symmetric formulation of the eigenvalue problem [32]. In equation (40), m and i start from 1 if $n > 1$.

The eigenvalue problem takes the following final form:

$$\mathbf{Ku} - \omega^2 \mathbf{Mu} = 0, \tag{42}$$

where

$$\mathbf{u}^{\mathrm{T}} = \{\mathbf{q}^{\mathrm{T}}, \mathbf{a}^{\mathrm{T}}\}, \tag{43}$$

$$\mathbf{K} = \begin{bmatrix} \mathbf{K}_P & \mathbf{0} \\ \mathbf{K}_1 & \mathbf{K}_S \end{bmatrix}, \qquad \mathbf{M} = \begin{bmatrix} \mathbf{M}_P & \mathbf{M}_F \\ \mathbf{0} & \mathbf{M}_S \end{bmatrix} \tag{44}$$

and ω is the circular frequency of vibration of the coupled system. If $n = 0$, the zero eigenvalue must be discarded. As a consequence of $\mathbf{K}_P$, $\mathbf{K}_S$, $\mathbf{M}_P$ and $\mathbf{M}_S$ being symmetric matrices and $\mathbf{K}_1 = -\mathbf{M}_F^{\mathrm{T}}$, the eigenvalue problem can easily be transformed into one for symmetric matrices [32]; this guarantees real eigenvalues.

6. NUMERICAL RESULTS AND DISCUSSION

Initially, numerical results have been obtained for some cases already theoretically and experimentally studied in the literature in order to validate the proposed method. Numerical results are then obtained for very flexible plates exhibiting full coupling between sloshing and bulging modes in order to examine this incompletely understood phenomenon and to show the potential of the method. The numerical results have been obtained by writing a code inside the *Mathematica* computer program [35]. If not specifically indicated, natural frequencies (Hz) are given as result; they correspond to $\omega/2\pi$, where ω is computed by using equation (42).

6.1. VALIDATION OF THE MODEL

The present model has been validated initially by comparison with the results of Bauer [23] for a clamped circular plate completely covering the fluid surface of a circular cylindrical tank. This system can be obtained as a special case of the present study by imposing $R = a$. The geometric and material properties of the system are: $R = 0{\cdot}5$ m, $a = 0{\cdot}5$ m, $h = 1$ mm, $\rho_P = 500$ kg/m^3, $\rho_F = 1000$ kg/m^3, $\nu = 0{\cdot}3$, $E = 1{\cdot}339 \times 10^{10}$ and $g = 9{\cdot}81$ m/s^2. Tables 1 and 2 show a comparison of the non-dimensional frequencies $\bar{\omega} = \omega a^2 \sqrt{\rho_P h/D}$ for different liquid levels H/a computed by using the present method and

TABLE 1

Comparison of the non-dimensional circular frequency $\bar{\omega} = \omega a^2 \sqrt{\rho_P h/D}$ *for the first three axisymmetric modes* ($n = 0$) *of clamped cover plates and different liquid levels* H/a *with data from Figure* 8 *in Bauer* [23]

Author	H/a	1st mode	2nd mode	3rd mode
Bauer [23]	0·1	1·7	5·9	13·8
Present study	0·1	1·52	5·79	13·83
Bauer [23]	1	2·5	7·5	15·9
Present study	1	2·40	7·37	15·82

TABLE 2

Comparison of the non-dimensional circular frequency $\bar{\omega} = \omega a^2\sqrt{\rho_P h/D}$ *for the first three asymmetric modes with one nodal diameter* ($n = 1$) *of clamped cover plates and different liquid levels* H/a *with data from Figure* 10 *in Bauer* [23]

Author	H/a	1st mode	2nd mode	3rd mode
Bauer [23]	0·1	0·69	3·3	9·3
Present study	0·1	0·52	3·18	9·21
Bauer [23]	1	1·5	4·8	11·3
Present study	1	1·10	4·54	11·14

TABLE 3

Comparison of the natural frequency (*Hz*) *of the bulging modes of simply supported plates of different thickness* h *with the data from Kwak* [25]

Author	n	h (mm)	1st mode	2nd mode
Kwak [25]	0	1	4·76	43·6
Present study	0	1	4·86	43·7
Kwak [25]	1	1	17·2	79·5
Present study	1	1	17·3	80·9
Kwak [25]	0	0·3	0·80	7·54
Present study	0	0·3	0·80	7·48
Kwak [25]	1	0·3	2·93	13·9
Present study	1	0·3	2·96	13·9

the data given in Bauer [23]. The agreement of the present results with those of Bauer [23] is good for both axisymmetric ($n = 0$) and asymmetric ($n = 1$) modes. Results have been obtained by using 10 terms in the expansion of the plate displacement and 50 terms in the expansion of the fluid velocity potential.

Another comparison has been performed between the present method and the results obtained by Kwak [25] for circular plates resting on the free surface of a half-infinite fluid domain. It must be specified that the results in Kwak [25] have been obtained by neglecting free-surface waves; therefore only natural frequencies of bulging modes can be compared. The dimensions R and H of the fluid domain are chosen to be large enough to approximate to a half-infinite domain. It must be observed that by increasing the ratio R/a, more terms are needed in the expansion of sloshing modes to reach a good degree of accuracy of the solution. The geometric and material properties of the system in this case are: $H = 2$ m, $R = 2$ m, $a = 0{\cdot}25$ m, $\rho_P = 7850\ \text{kg/m}^3$, $\rho_F = 1000\ \text{kg/m}^3$, $v = 0{\cdot}3$, $E = 2{\cdot}06 \times 10^{11}$ and $g = 9{\cdot}81\ \text{m/s}^2$. The thickness h is given in Table 3. A good agreement between bulging frequencies obtained by using the present method and those of Kwak is observed; in fact in this case the dimensions of the plate and fluid domain give results close to those for a half-infinite fluid domain. However, sloshing frequencies cannot be studied by using the method proposed by Kwak. In the following section, it will be shown that sloshing and bulging modes are largely coupled for very flexible plates and the study of their coupling is fundamental in this case.

A comparison between the experimental results obtained by Kwak and Han [28] for a free-edge circular plate resting on the water surface has also been performed; the water

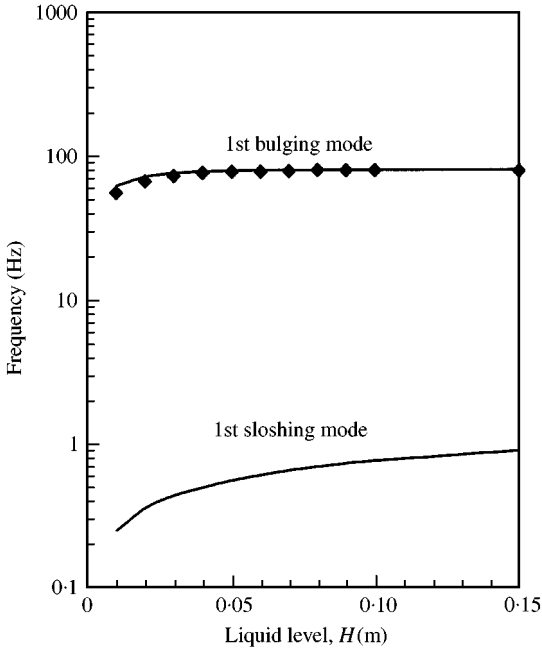

Figure 2. Natural frequencies of the first sloshing and bulging modes with $n = 2$ nodal diameters; case of Kwak and Han [28]. ——, present theoretical results; ◆, experimental values from reference [28].

was contained in a circular cylindrical tank where the plate was suspended by a string. The geometric and material properties of the test system of Kwak and Han [28] were $R = 0{\cdot}6$ m, $a = 0{\cdot}15$ m, $\rho_P = 7730$ kg/m^3, $\rho_F = 1000$ kg/m^3, $\nu = 0{\cdot}3$, $E = 2{\cdot}1 \times 10^{11}$; H was varied. Only bulging modes are reported in reference [28] where theoretical results are also reported, obtained by neglecting free-surface waves and considering an infinite water domain in the radial direction. Figure 2 presents a comparison of the fundamental bulging mode of the plate, having $n = 2$ nodal diameters. The agreement between the present theoretical results and experiments is very good. Figure 3 presents a comparison of the first axisymmetric bulging mode of the plate, being the second bulging mode of the system. In this case the agreement is less; however the theoretical and experimental results show a similar trend. Theoretical results obtained by Kwak and Han [28] also present a similar difference in this case.

6.2. RESULTS FOR FULLY COUPLED SLOSHING AND BULGING MODES

In the previous section, the present model and the relative computer code, give results which are in good agreement with the data available in the literature. It has also been shown that different problems can be obtained as limiting cases of the studied problem. In this section, free vibrations of the system are studied for very flexible plates that present bulging modes with natural frequencies very close to those of sloshing modes. In this case, a very strong interaction between sloshing and bulging modes arises, changing mode shapes and frequencies of the uncoupled system. In particular, sloshing modes are associated with a significant vibration amplitude of the plate; similarly, bulging modes of the plate are associated with a significant amplitude of free-surface waves.

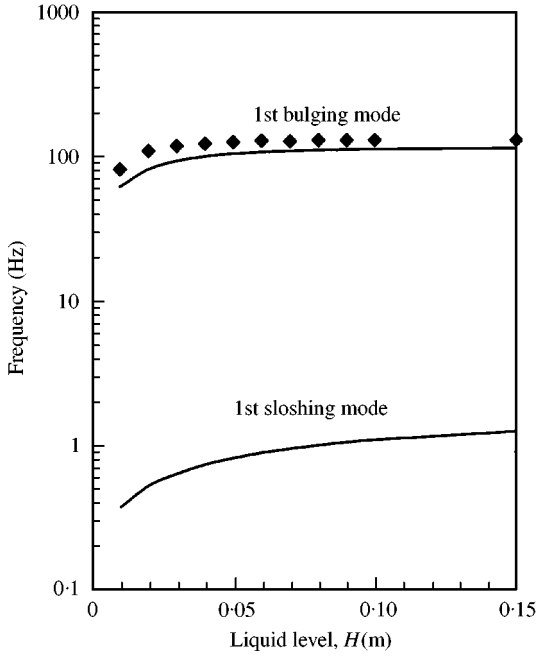

Figure 3. Natural frequencies of the first sloshing and bulging modes with $n = 0$ nodal diameters (axisymmetric mode); case of Kwak and Han [28]. ——, present theoretical results; ◆, experimental values from reference [28].

TABLE 4

Convergence of the solution with the number of terms N_1 and N_2 in the plate and fluid expansions, respectively; $h = 1$ *mm*, $a = 0{\cdot}25$ *m*, $n = 0$, $H = 0{\cdot}3$ *m*, $R = 0{\cdot}5$ *m*

N_1	N_2	1st S mode	2nd S mode	1st B mode	2nd B mode
4	10	1·84	2·56	4·64	40·0
5	25	1·84	2·56	4·82	44·1
10	50	1·84	2·56	4·82	43·4
20	50	1·84	2·56	4·82	43·4
10	100	1·80	2·57	4·82	43·6
10	150	1·78	2·58	4·82	43·7

Initially a system with the following geometric and material characteristics has been studied: $H = 0{\cdot}3$ m, $R = 0{\cdot}5$ m, $a = 0{\cdot}25$ m, $h = 1$ mm, $\rho_P = 7850$ kg/m^3, $\rho_F = 1000$ kg/m^3, $v = 0{\cdot}3$, $E = 2{\cdot}06 \times 10^{11}$. Table 4 shows the convergence of the solution versus the number of terms in the expansion of the plate displacement and fluid potential. Table 4 shows that 10 terms for the plate displacement and 50 terms for the fluid potential are enough to give good accuracy of the natural frequencies. However, a more specific discussion on the convergence of mode shape is deferred to the last part of this section.

Figure 4 gives the natural frequencies of the first sloshing and bulging modes versus the number n of nodal diameters of the free-edge plate with the same system characteristics previously given for Table 4, except for a reduced thickness $h = 0{\cdot}3$ mm. It is clearly shown that the fundamental sloshing modes has one nodal diameter and that the fundamental

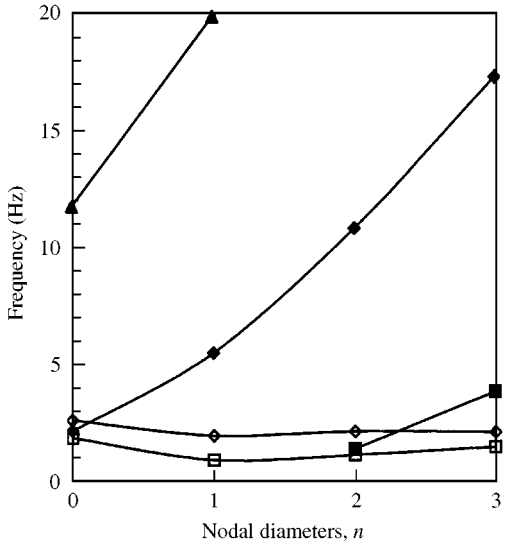

Figure 4. Natural frequencies of the first two sloshing modes and of bulging modes with $m = 0$, 1, 2 circular nodes versus the number n of nodal diameters; free-edge plate, $h = 0{\cdot}3$ mm. —□—, 1st sloshing mode; —◇—, 2nd sloshing mode; —■—, bulging mode with $m = 0$; —◆—, bulging mode with $m = 1$; —▲—, bulging mode with $m = 2$.

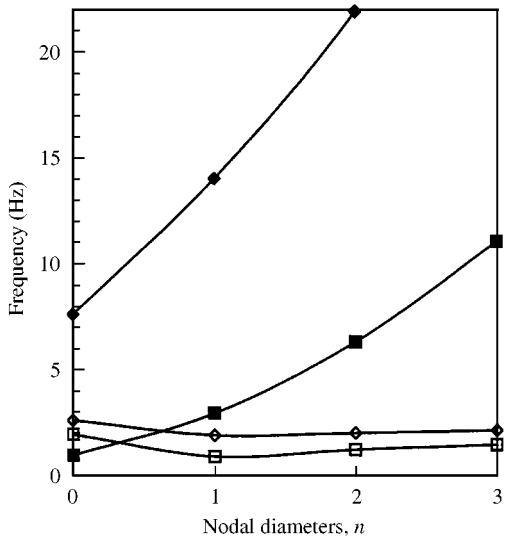

Figure 5. Natural frequencies of the first two sloshing modes and of bulging modes with $m = 0$, 1 circular nodes versus the number n of nodal diameters; simply supported plate, $h = 0{\cdot}3$ mm. —□—, 1st sloshing mode; —◇—, 2nd sloshing mode; —■—, bulging mode with $m = 0$; —◆—, bulging mode with $m = 1$.

bulging mode has two nodal diameters. In particular, for $n = 0$ and 2 the first sloshing and bulging modes are very close in frequency and largely coupled; in the last part of this section mode shapes are given showing this coupling.

Figure 5 is similar to Figure 4 but applies to a simply supported plate; all the other system parameters are the same as those in Figure 4. In this case, the fundamental sloshing

mode still has one nodal diameter but the fundamental bulging mode has zero nodal diameters.

The effect of the level of the liquid below the plate is investigated in Figure 6. The plate has a thickness $h = 1$ mm and is simply supported; all the other system parameters remain unchanged; axisymmetric modes ($n = 0$) are investigated. The water level H is varied between 0·005 and 1 m. It is interesting to note that an increment of the water level from 0·4 to 1 m has almost no effect on the natural frequencies. Otherwise, in the range between 0·005 and 0·2 m, a change of the liquid level has an important effect on the natural frequencies of the sloshing and bulging modes.

The effect of the radial dimension of the container is studied in Figure 7. All parameters and boundary conditions are the same as in Figure 6, but the water level is fixed, $H = 0{\cdot}5$ m, and the radius R is varied from 0·25 m (where $R = a$) to 2 m. In this case, the natural frequency of bulging modes remain almost unaffected when the radius R is increased over the value $2a$; but this is not verified by sloshing modes. However, for both the sloshing and bulging modes, the largest change in the frequency is obtained when R is varied in the range $a \leqslant R \leqslant 2a$. In Figure 7, it is to be noted that the sloshing modes disappear for $R = a$ as a consequence that all the liquid is covered by the floating plate in this case, and that the fundamental mode of the system becomes the bulging mode with 1 nodal circle. In fact, the bulging mode without nodal circles ($m = 0$) is no longer possible due to the conservation of the fluid volume.

The sloshing and bulging mode shapes of axisymmetric modes ($n = 0$) of the simply supported plate of thickness $h = 1$ mm ($R = 0{\cdot}5$ m and $H = 0{\cdot}3$ m) are given in Figure 8. Both the plate and liquid surface displacements are plotted. This allows the convergence of the method to be checked since the liquid surface and plate displacement should be the same for $0 \leqslant r \leqslant a = 0{\cdot}25$ m. It is clear that the convergence of mode shapes, which is actually slower than the convergence of frequencies, is very good with 10 terms for the plate displacement and 50 terms for the fluid potential, except for the second bulging mode (see Figure 8(d)). For this mode, more sloshing modes must be included in the expansion for the

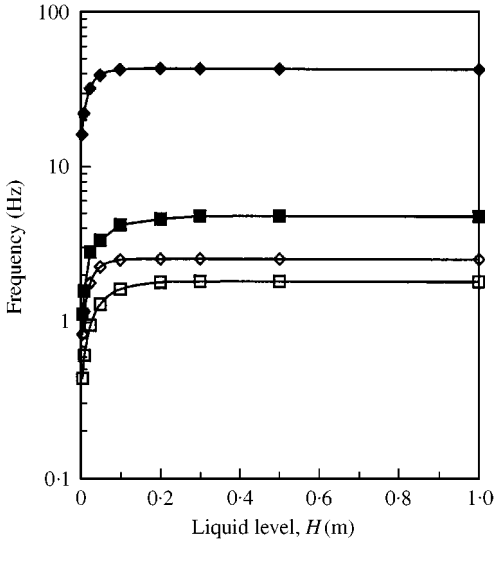

Figure 6. Natural frequencies of the first two sloshing and bulging modes with $n = 0$ nodal diameters (axisymmetric modes) versus the liquid level H; simply supported plate, $h = 1$ mm, $R = 0{\cdot}5$ m. —□—, 1st sloshing mode; —◇—, 2nd sloshing mode; —■—, bulging mode with $m = 0$; —◆—, bulging mode with $m = 1$.

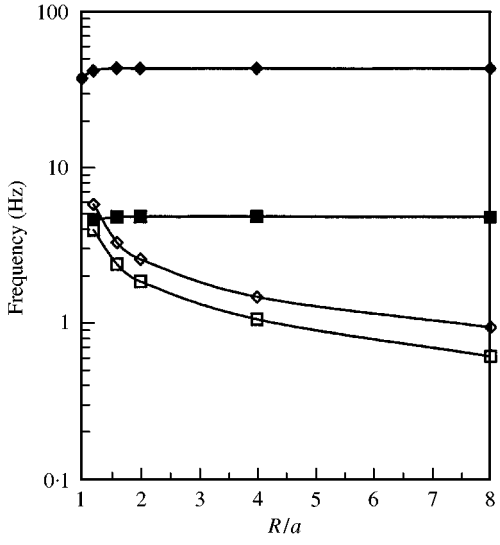

Figure 7. Natural frequencies of the first two sloshing and bulging modes with $n = 0$ nodal diameters (axisymmetric modes) versus the ratio R/a; simply supported plate, $h = 1$ mm, $H = 0{\cdot}5$ m. —□—, 1st sloshing mode; —◇—, 2nd sloshing mode; —■—, bulging mode with $m = 0$; —◆—, bulging mode with $m = 1$.

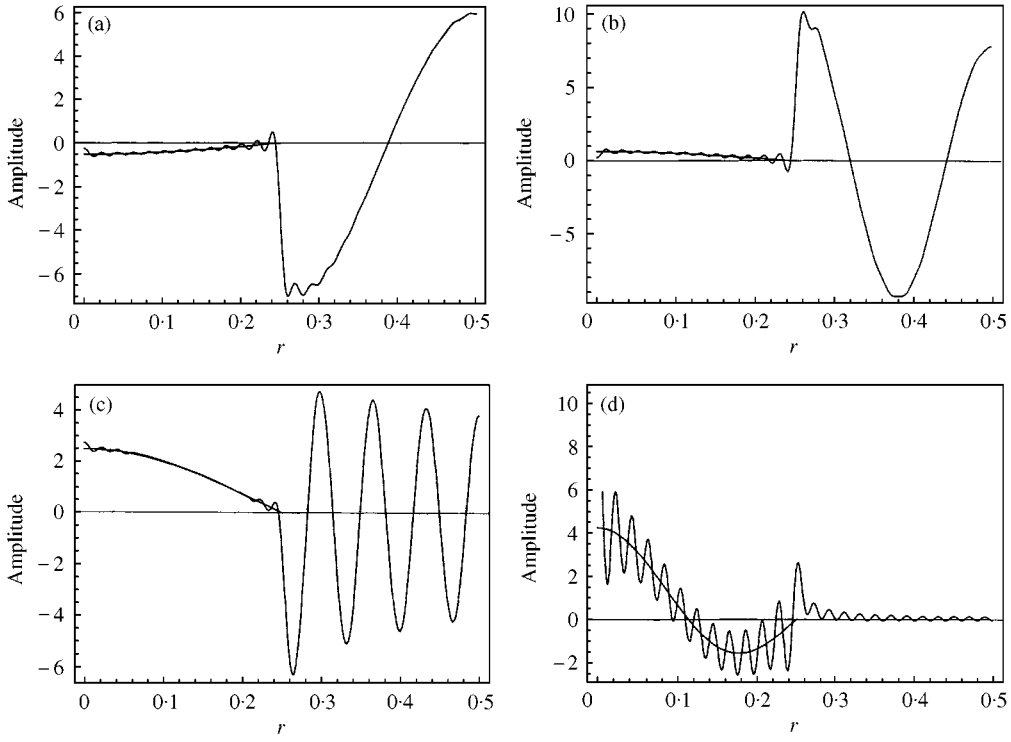

Figure 8. Mode shapes of the first two sloshing and bulging modes with $n = 0$ nodal diameters (axisymmetric modes); simply supported plate, $h = 1$ mm, $R = 0{\cdot}5$ m, $H = 0{\cdot}3$ m. (a) 1st sloshing mode, 1·84 Hz; (b) 2nd sloshing mode, 2·56 Hz; (c) 1st bulging mode, 4·82 Hz; (d) 2nd bulging mode, 43·4 Hz.

convergence of the mode shape (actually the natural frequency already reached convergence in this case). This point is discussed at the end of this section. It is interesting to observe that a significant plate displacement is observed for the sloshing modes. Moreover, the amplitude of free surface waves for the bulging modes is even larger than the plate displacement (see Figure 8(c)).

The sloshing and bulging mode shapes of the same plate but with the thickness reduced to $h = 0{\cdot}3$ mm are given in Figure 9. In this case the convergence of mode shapes, with the same number of terms, is better than in the previous case because the sloshing and bulging modes are closer in frequency, especially for the second bulging modes. In this case, the first axisymmetric bulging mode has a lower frequency than the one of the first axisymmetric sloshing mode. For this reason, the amplitude of the free-surface oscillations coupled to the first bulging mode (see Figure 9(c)) are smaller than in Figure 8(c). A larger plate displacement is associated with sloshing modes with respect to Figure 8(a) and (b) because the plate is more flexible.

The same plate studied in Figure 9 is analyzed in Figure 10, but with mode shapes having one nodal diameter ($n = 1$). Figures 10(a)–(d) have been calculated with 10 terms for the plate displacement and 50 terms for the fluid potential; convergence is good except for the second bulging mode, as discussed in Figure 8. In fact, the 50th sloshing mode does not reach the natural frequency of the second bulging modes. Figure 10(e) presents the second bulging modes calculated with 10 terms for the plate displacement and 200 terms for the fluid potential; a good convergence is reached in this case on the plate surface. In this case the 200th sloshing modes has a natural frequency higher than that for the second bulging mode. However, the difference in frequency between the computations in Figures 10(d) and (e) is negligible, as indicated in the figure caption.

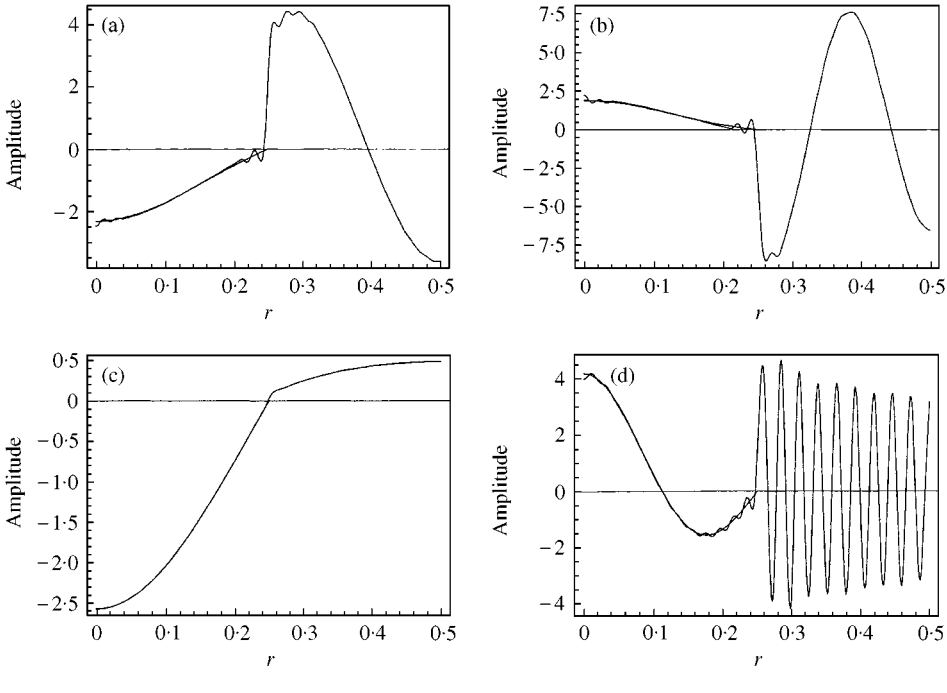

Figure 9. Mode shapes of the first two sloshing and bulging modes with $n = 0$ nodal diameters (axisymmetric modes); simply supported plate, $h = 0{\cdot}3$ mm, $R = 0{\cdot}5$ m, $H = 0{\cdot}3$ m. (a) 1st sloshing mode, 1·93 Hz; (b) 2nd sloshing mode, 2·60 Hz; (c) 1st bulging mode, 0·95 Hz; (d) 2nd bulging mode, 7·62 Hz.

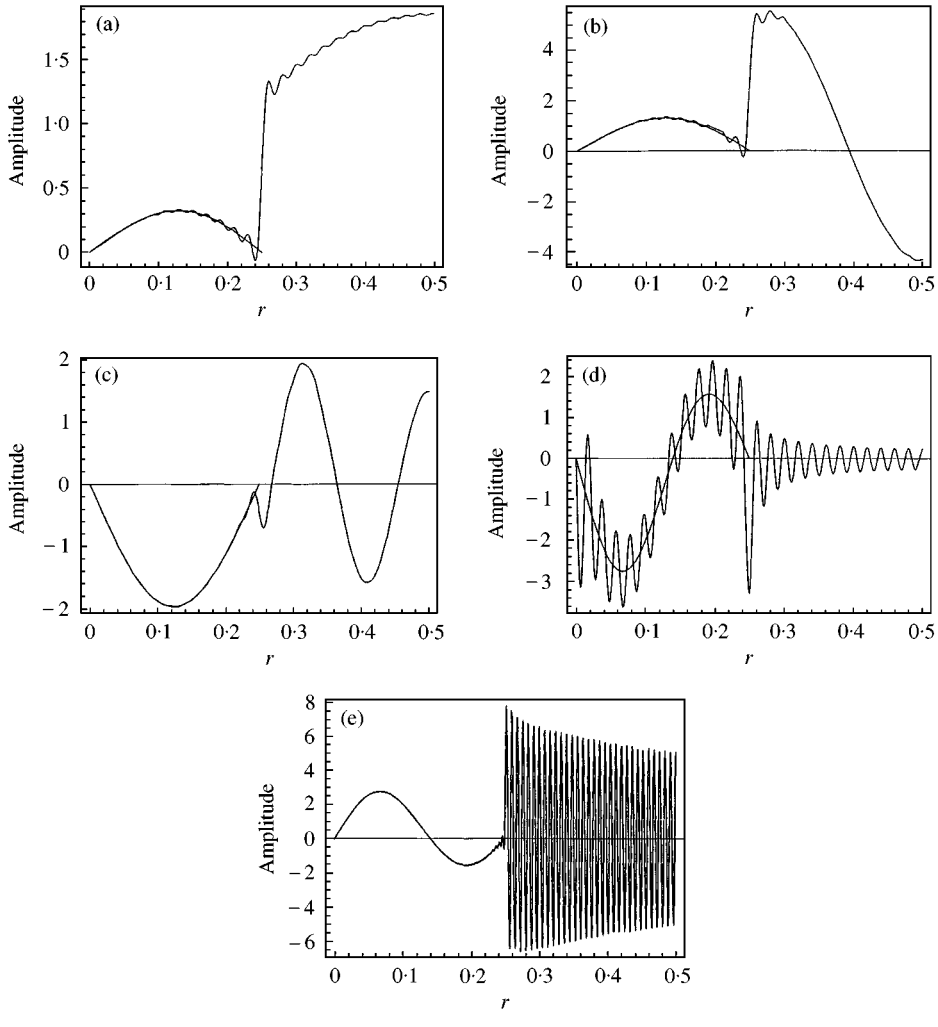

Figure 10. Mode shapes of the first two sloshing and bulging modes with $n = 1$ nodal diameter; simply supported plate, $h = 0{\cdot}3$ mm, $R = 0{\cdot}5$ m, $H = 0{\cdot}3$ m. (a) 1st sloshing mode, 0·88 Hz; (b) 2nd sloshing mode, 1·89 Hz; (c) 1st bulging mode, 2·93 Hz; (d) 2nd bulging mode, 14·04 Hz, computed with $N_1 = 10$ plate terms and $N_2 = 50$ fluid terms; (e) 2nd bulging mode, 13·98 Hz, computed with $N_1 = 10$ plate terms and $N_2 = 200$ fluid terms.

In general, the sloshing modes must cover the frequency range of the bulging modes analyzed in order to calculate the mode shape of the free-surface waves accurately. This is an interesting result. Similarly, by using a classical finite element code, a very refined mesh must be used to discretize the free surface of the fluid to calculate the free-surface waves. Figure 10(e) shows how many waves are obtained on the free surface; not less than two nodes per wave should be used to reconstruct the free-surface waves.

The problem investigated in Figures 8 and 9 was studied by varying the plate thickness in Figure 11. This figure shows that a larger interaction between the first bulging and sloshing modes arises for a plate thickness around $h = 0{\cdot}5$ mm. However, for thinner plates, the interaction between the sloshing and bulging modes is fundamental. Only when the plate thickness is large enough does the sloshing and bulging vibrations become practically uncoupled.

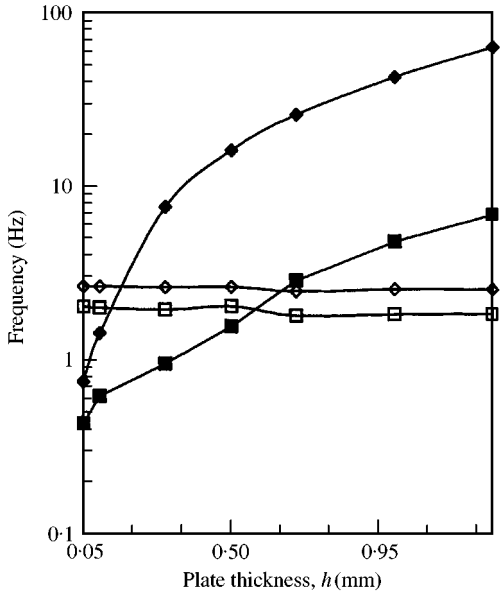

Figure 11. Natural frequencies of the first two sloshing and bulging modes with $n = 0$ nodal diameters (axisymmetric modes) versus the plate thickness h; simply supported plate, $R = 0{\cdot}5$ m, $H = 0{\cdot}3$ m. —□—, 1st sloshing mode; —◇—, 2nd sloshing mode; —■—, 1st bulging mode; —◆—, 2nd bulging mode.

7. CONCLUSIONS

The present study introduces a new solution for the vibrations of circular plates resting on a free liquid surface. The method enables plates with a very strong coupling between the sloshing and bulging modes to be studied accurately. Free vibrations are studied numerically in cases of very flexible plates that present bulging modes with natural frequencies very close to those of the sloshing modes. In these cases, a very strong interaction between the sloshing and bulging modes arises. Significant plate displacement is observed for the sloshing modes. Moreover, the amplitude of the free-surface waves for the bulging modes can even be larger than the plate displacement.

When the distance of rigid surfaces containing the water from the plate is increased (or deceased) to a value larger than twice the plate radius (both in radial and axial directions), no significant effect has been found on the frequency of the bulging modes of simply supported plates. However, if the distance of these rigid surfaces from the plate is reduced the effect on natural frequencies can be very important.

ACKNOWLEDGMENTS

This research was partially supported by the Italian Space Agency (ASI).

REFERENCES

1. Lord Rayleigh 1945 *Theory of Sound*. New York: Dover; second edition (1st ed. 1877).
2. H. Lamb 1921 *Proceedings of the Royal Society* (*London*) **A98**, 205–216. On the vibrations of an elastic plate in contact with water.

3. N. W. McLachlan 1932 *Proceedings of the Physical Society* (*London*) **44**, 546–555. The accession to inertia of flexible discs vibrating in a fluid.
4. M. Amabili and M. K. Kwak 1996 *Journal of Fluids and Structures* **10**, 743–761. Free vibration of circular plates coupled with liquids: revising the Lamb problem.
5. M. Amabili 1996 *Journal of Sound and Vibration* **193**, 909–925. Effect of finite fluid depth on the hydroelastic vibrations of circular and annular plates.
6. M. Amabili, G. Frosali and M. K. Kwak 1996 *Journal of Sound and Vibration* **191**, 825–846. Free vibrations of annular plates coupled with fluids.
7. J. H. Ginsberg and P. Chu 1992 *Journal of the Acoustical Society of America* **91**, 894–906. Asymmetric vibration of a heavily fluid-loaded circular plate using variational principles.
8. G. Butha and L. R. Koval 1964 *Journal of the Acoustical Society of America* **36**, 2071–2079. Hydroelastic solution of the sloshing of a liquid in a cylindrical tank.
9. P. Tong 1967 *American Institute of Aeronautics and Astronautics Journal* **5**, 1842–1848. Liquid motion in a cyrcular cylindrical container with a flexible bottom.
10. J. Siekmann and S. C. Chang 1968 *Ingenieur Archiv* **37**, 99–109. On the dynamics of liquid in a cylindrical tank with a flexible bottom.
11. H. F. Bauer, T.-M. Hsu and J. T.-S. Wang 1968 *Transactions of the American Society of Mechanical Engineers*, *Journal of Basic Engineering* Series D **90**, 373–377. Interaction of a sloshing liquid with elastic containers.
12. H. F. Bauer, S. S. Chang and J. T. S. Wang 1971 *American Institute of Aeronautics and Astronautics Journal* **9**, 2333–2339. Nonlinear liquid motion in a longitudinal excited container with elastic bottom.
13. H. F. Bauer and J. Siekmann 1971 *Ingenieur Archiv* **40**, 266–280. Dynamic interaction of a liquid with the elastic structure of a circular cylindrical container.
14. K. Nagaya and K. Nagai 1986 *Journal of Sound and Vibration* **70**, 333–345. Dynamic response of circular plates in contact with a fluid subjected to general dynamic pressures on a fluid surface.
15. M. Chiba 1992 *Journal of Fluids and Structures* **6**, 181–206. Nonlinear hydroelastic vibration of a cylindrical tank with an elastic bottom, containing liquid. Part I: experiment.
16. M. Chiba 1993 *Journal of Fluids and Structures* **7**, 57–73. Nonlinear hydroelastic vibration of a cylindrical tank with an elastic bottom, containing liquid. Part II: linear axisymmetric vibration analysis.
17. M. Chiba 1996 *International Journal of Non-Linear Mechanics* **31**, 155–165. Non-linear hydroelastic vibration of a cylindrical tank with an elastic bottom containing liquid—III. Non-linear analysis with Ritz averaging method.
18. M. Chiba and K. Abe 1999 *Thin-Walled Structures* **34**, 233–260. Nonlinear hydroelastic vibration of a cylindrical tank with an elastic bottom containing liquid—analysis using harmonic balance method.
19. M. Chiba 1994 *Journal of Sound and Vibration* **169**, 387–394. Axisymmetric free hydroelastic vibration of a flexural bottom plate in a cylindrical tank supported on an elastic foundation.
20. M. Amabili 1997 *Shock and Vibration* **4**, 51–68. Bulging modes of circular bottom plates in rigid cylindrical containers filled with a liquid.
21. M. Amabili and G. Dalpiaz 1998 *Journal of Sound and Vibration* **210**, 329–350. Vibrations of base plates in annular cylindrical tanks: theory and experiments.
22. M. Amabili, M. P. Païdoussis and A. A. Lakis 1998 *Journal of Sound and Vibration* **213**, 259–299. Vibrations of partially filled cylindrical tanks with ring-stiffeners and flexible bottom.
23. H. F. Bauer 1995 *Journal of Sound and Vibration* **180**, 689–704. Coupled frequencies of a liquid in a circular cylindrical container with elastic liquid surface cover.
24. M. K. Kwak and K. C. Kim 1991 *Journal of Sound and Vibration* **146**, 381–389. Axisymmetric vibration of circular plates in contact with fluid.
25. M. K. Kwak 1991 *Transactions of the American Society of Mechanical Engineers*, *Journal of Applied Mechanics* **58**, 480–483. Vibration of circular plates in contact with water.
26. M. Amabili, G. Dalpiaz and C. Santolini 1995 *Modal Analysis*: *The International Journal of Analytical and Experimental Modal Analysis* **10**, 187–202. Free-edge circular plates vibrating in water.
27. M. K. Kwak and M. Amabili 1999 *Transactions of the American Soceity of Mechanical Engineers*, *Journal of Vibration and Acoustics* **121**, 26–32. Hydroelastic vibration of free-edge annular plates.
28. M. K. Kwak and S.-B. Han 2000 *Journal of Sound and Vibration* **230**, 171–185. Effect of fluid depth on the hydroelastic vibration of free-edge circular plate.
29. M. Amabili and M. K. Kwak 1999 *Journal of Sound and Vibration* **226**, 407–424. Vibration of circular plates on a free fluid surface: effect of surface waves.

30. D. WHEELON 1968 *Tables of Summable Series and Integrals Involving Bessel Functions.* San Francisco: Holden-Day.
31. I. S. GRADSHTEYN and I. M. RYZHIK 1994 *Table of Integrals, Series and Products.* London: Academic Press; fifth edition.
32. M. AMABILI 2000 *Journal of Sound and Vibration* **231**, 79–97. Eigenvalue problems for vibrating structures coupled with quiescent fluids with free surface.
33. M. AMABILI 1997 *Journal of Fluids and Structures* **11**, 507–523. Ritz method and substructuring in the study of vibration with strong fluid-structure interaction.
34. H. LAMB 1945 *Hydrodynamics.* New York: Dover. p. 46.
35. S. WOLFRAM 1999 *The Mathematica Book*. Cambridge, UK: Cambridge University Press; fourth edition.

APPENDIX A: FREQUENCY AND MODE-SHAPE PARAMETERS

The frequency parameters of circular plates with clamped, simply supported, and free-edge boundary conditions can be obtained by solving the characteristic equations:

$$\mathrm{J}_n(\lambda_{nm})\,\mathrm{I}_{n+1}(\lambda_{nm}) + \mathrm{I}_n(\lambda_{nm})\,\mathrm{J}_{n+1}(\lambda_{nm}) = 0 \quad \text{for a clamped circular plate,}$$

$$\frac{\mathrm{J}_{n+1}(\lambda_{nm})}{\mathrm{J}_n(\lambda_{nm})} + \frac{\mathrm{I}_{n+1}(\lambda_{nm})}{\mathrm{I}_n(\lambda_{nm})} = \frac{2\lambda_{nm}}{1-\nu} \quad \text{for a simply supported circular plate}$$

and

$$\frac{\lambda_{nm}^2\,\mathrm{J}_n(\lambda_{nm}) + (1-\nu)\,[\lambda_{nm}\,\mathrm{J}'_n(\lambda_{nm}) - n^2\,\mathrm{J}_n(\lambda_{nm})]}{\lambda_{nm}^2\,\mathrm{I}_n(\lambda_{nm}) - (1-\nu)[\lambda_{nm}\,\mathrm{I}'_n(\lambda_{nm}) - n^2\,\mathrm{I}_n(\lambda_{nm})]}$$

$$= \frac{\lambda_{nm}^3\,\mathrm{J}'_n(\lambda_{nm}) + (1-\nu)\,n^2\,[\lambda_{nm}\,\mathrm{J}'_n(\lambda_{nm}) - \mathrm{J}_n(\lambda_{nm})]}{\lambda_{nm}^3\,\mathrm{I}'_n(\lambda_{nm}) - (1-\nu)n^2\,[\lambda_{nm}\,\mathrm{I}'_n(\lambda_{nm}) - \mathrm{I}_n(\lambda_{nm})]} \quad \text{for a free-edge circular plate,}$$

where J'_n and I'_n indicate the derivatives of Bessel functions with respect to the argument.

The mode-shape parameters can be calculated by using the equations

$$\frac{C_{nm}}{A_{nm}} = -\frac{\mathrm{J}_n(\lambda_{nm})}{\mathrm{I}_n(\lambda_{nm})} \quad \text{for a clamped and simply supported circular plate}$$

and

$$\frac{C_{nm}}{A_{nm}} = \frac{\lambda_{nm}^2\,\mathrm{J}_n(\lambda_{nm}) + (1-\nu)\,[\lambda_{nm}\,\mathrm{J}'_n(\lambda_{nm}) - n^2\,\mathrm{J}_n(\lambda_{nm})]}{\lambda_{nm}^2\,\mathrm{I}_n(\lambda_{nm}) - (1-\nu)[\lambda_{nm}\,\mathrm{I}'_n(\lambda_{nm}) - n^2\,\mathrm{I}_n(\lambda_{nm})]} \quad \text{for a free-edge circular plate.}$$

TABLE A1

Frequency parameters λ_{nm} for clamped circular plates

m	$n=0$	$n=1$	$n=2$	$n=3$	$n=4$	$n=5$
0	3·1962	4·6109	5·9059	7·1442	8·3466	9·5257
1	6·3064	7·7987	9·2114	10·5361	11·8367	13·1074
2	9·4395	10·9581	12·4020	13·7949	15·1499	16·4751
3	12·5771	14·1089	15·5792	17·0050	18·3960	19·7583
4	15·7164	17·2560	18·7451	20·1921	21·6084	22·9979
5	18·8565	20·4010	21·9009	23·3660	24·8015	26·2117

TABLE A2

Frequency parameters λ_{nm} for simply supported circular plates ($\nu = 0{\cdot}3$)

m	$n = 0$	$n = 1$	$n = 2$	$n = 3$	$n = 4$	$n = 5$
0	2·2215	3·7280	5·0610	6·3212	7·5393	8·7294
1	5·4516	6·9627	8·3736	9·7236	11·0319	12·3093
2	8·6114	10·1377	11·5887	12·9875	14·3475	15·6773
3	11·7609	13·2967	14·7717	16·2014	17·5957	18·9613
4	14·9069	16·4489	17·9399	19·3910	20·8098	22·2018
5	18·0513	19·5977	21·1001	22·5670	24·0042	25·4164

TABLE A3

Frequency parameters λ_{nm} for free-edge circular plates ($\nu = 0{\cdot}3$)

m	$n = 0$	$n = 1$	$n = 2$	$n = 3$	$n = 4$	$n = 5$
0	—	—	2·3148	3·5269	4·6728	5·7875
1	3·0005	4·5249	5·9380	7·2806	8·5757	9·8364
2	6·2003	7·7338	9·1851	10·5804	11·9344	13·2565
3	9·3675	10·9068	12·3817	13·8091	15·1997	16·5606
4	12·5227	14·0667	15·5575	17·0070	18·4232	19·8117
5	15·6727	17·2203	18·7226	20·1882	21·6234	23·0330

The frequency parameters λ_{nm} are given in Tables A1–A3 for n and m up to five, for free-edge, simply supported and clamped plates.

APPENDIX B: NOMENCLATURE

a	plate radius
D	flexural stiffness of the plate
E	Young's modulus of the plate material
g	gravity acceleration
h	plate thickness
H	level of the liquid
I_n	modified Bessel function of order n
J_n	Bessel function of order n
m	number of nodal diameters
n	number of nodal circles
q_m	Ritz coefficient
$\mathbf{q}$	vector of Ritz coefficients
r	radial co-ordinate
R	internal radius of the container
t	time
T_F^*	reduced reference kinetic energy of the liquid
T_P^*	reference kinetic energy of the plate
V_P	maximum potential energy of the plate
w	deflection of the plate
W_{nm}	radial mode shape function
z	co-ordinate along the tank axis
θ	angular co-ordinate

λ_{nm} plate frequency parameter
Φ spatial velocity potential of the liquid
v Poisson ratio
ρ_F mass density of the liquid
ρ_P mass density of the plate material
ω radian frequency of the plate–liquid system (rad/s)
ω_{nm} radian frequency of the plate in vacuo (rad/s)
$\bar{\omega}$ non-dimensional frequency
∇^2 Laplace operator